hep-ph/9904319
FTUV-97/51
IFIC-97/82
PRL-TH-97/28
ITP-SB-97-67

Longitudinal quark polarization in $e^+e^- \to t\bar{t}$ and chromoelectric and chromomagnetic dipole couplings of the top quark

Saurabh D. Rindani[a] and Michael M. Tung[b]

Instituto de Física Corpuscular, Departament de Física Teòrica
Universitat de València, 46100 Burjassot (València), Spain

[a] *Theory Group, Physical Research Laboratory*
Navrangpura, Ahmedabad 380 009, India

[b] *Institute for Theoretical Physics*
State University of New York
Stony Brook, NY 11794-3840, U.S.A

Abstract

The effect of anomalous chromomagnetic (μ) and chromoelectric couplings (d) of the gluon to the top quark are considered in $e^+e^- \to t\bar{t}$, with unpolarized and longitudinally polarized electron beams. The total cross section, as well as t and $\bar{t}$ polarizations are calculated to order α_s in the presence of the anomalous couplings. One of the two linear combinations of t and $\bar{t}$ polarizations is CP even, while the other is CP odd. The limits that could be obtained at a typical future linear collider with an integrated luminosity of 50 fb^{-1} and a total c.m. energy of 500 GeV on the most sensitive CP-even combination of anomalous couplings are estimated as $-3 < \mathrm{Re}(\mu) < 2$, for $\mathrm{Im}(\mu) = 0 = d$ and $\sqrt{\mathrm{Im}(\mu)^2 + |d|^2} < 2.25$ for $\mathrm{Re}(\mu) = 0$. There is an improvement by roughly a factor of 2 at 1000 GeV. On the other hand, from the CP-odd combination, we derive the possible

complementary bounds as $-3.6 < \mathrm{Im}(\mu^* d) < 3.6$ for $\mathrm{Im}(d) = 0$ and $-10 < \mathrm{Im}(d) < 10$ for $\mathrm{Im}(\mu^* d) = 0$, for a c.m. energy of 500 GeV. The corresponding limit for 1000 GeV is almost an order of magnitude better for $\mathrm{Im}(\mu^* d)$, though somewhat worse for $\mathrm{Im}(d)$. Results for the c.m. energies 500 GeV and 1000 GeV, if combined, would yield *independent* limits on the two CP-violating parameters of $-0.8 < \mathrm{Im}(\mu^* d) < 0.8$ and $-11 < \mathrm{Im}(d) < 11$.

PACS numbers: 12.38.Bx, 13.40.Em, 13.88.+e, 14.65.HA

1 Introduction

The discovery of a heavy top quark, with a mass of $m_t = 175 \pm 6$ GeV [1], which is far larger than that of all other quarks, opens up the possibility that the top quark may have properties very different from those of the other quarks. Observation of these properties might even signal new physics beyond the standard model. Several efforts in the past few years have gone into the investigation of the potential of different experiments to study possible new interactions of the top quark. In particular, possible anomalous couplings of the top quark to electroweak gauge bosons[1] and to gluons [3, 4] have also been discussed. Top polarization is especially useful in such studies [5, 6, 7, 8], because with a mass around 175 GeV, the top quark decays before it can hadronize [9], and all spin information is preserved in the decay distributions.

In this paper, we investigate the potential of e^+e^- experiments at a future linear collider with centre-of-mass (c.m.) energies of 500 GeV or higher, to study anomalous chromomagnetic and chromoelectric dipole couplings of the top quark to gluons. So far, a considerable amount of earlier work on the topic of anomalous gluon couplings has concentrated on hadron colliders. But also high energy e^+e^- experiments with sufficiently high luminosities would provide a relatively clean environment to probe the standard model for anomalous gluon couplings. While earlier efforts in the context of e^+e^- colliders are mainly based on an analysis of the gluon distribution [4] in $e^+e^- \to t\bar{t}g$, we look at the possible information that could be obtained from studying the total cross section, and the polarization of t and $\bar{t}$ separately. This has the advantage over t and $\bar{t}$ spin correlations that, because the polarization of only one of t and $\bar{t}$ is analyzed by means of a definite decay channel, the other is free to decay into any channel. This leads to much better statistics compared to the case when $t-\bar{t}$ spin correlations are considered, where definite t and $\bar{t}$ channels have to be used as analyzers.

We find that there are three independent quantities, viz., the cross section, and the CP-even and CP-odd linear combinations of the t and $\bar{t}$ polarizations, which can be used to

[1] References to the voluminous literature on this subject can be found, for example, in [2].

probe separately the CP-even chromomagnetic dipole moment coupling and the CP-odd chromoelectric dipole coupling. Of these, the CP-odd combination provides the most sensitive probe of the imaginary parts of the anomalous couplings.

We obtain here the 90% confidence level (C.L.) limits that would be possible at a typical e^+e^- linear collider, with integrated luminosity 50 fb^{-1}. We have considered two possible centre-of-mass (c.m.) energies, viz., 500 GeV and 1000 GeV. We have also considered the effect of beam polarization on the sensitivity of the measurements.

Our results on the constraints on the CP-violating chromoelectric dipole moments were presented in Ref. [10] . We include in this paper also the limits that would be obtainable on CP-conserving chromomagnetic dipole moments, and combinations of couplings.

The paper is organized as follows: In Section 2, we introduce the effective action for the general massive anomalous $q\bar{q}g$ vertex. The subsequent discussion presents the full framework necessary for obtaining the analytical extensions that modify the standard QCD one-loop predictions for quark-antiquark production. We then give explicit combinations of the total polarized cross sections which are sensitive to the chromomagnetic and chromoelectric dipole moments, respectively. Next, Section 3 focuses on the numerical estimates of these observables for various kinematical regions readily accessible at a future e^+e^- collider. The final Section 4 is the Conclusion.

2 Calculation of cross section and top polarization with anomalous couplings

An effective $t\bar{t}g$ vertex can be written in the form

$$\Gamma^a_{t\bar{t}g} = -g_s T^a \left[\gamma^\mu \epsilon_\mu + \frac{i\mu}{m_t}\sigma^{\mu\nu} q_\mu \epsilon_\nu - \frac{d}{m_t}\sigma^{\mu\nu}\gamma_5 q_\mu \epsilon_\nu\right], \tag{1}$$

where

$$T^a = \tfrac{1}{2}\lambda^a; \tag{2}$$

λ^a being the $SU(3)$ Gell-Mann matrices, and q_μ and ϵ_μ are respectively the momentum and polarization four-vectors of the gluon. This is the most general Lorentz- and colour-invariant trilinear coupling (additional quadrilinear terms are needed for local colour invariance, but we do not need them here). The μ and d terms are the chromomagnetic and chromoelectric dipole terms, respectively. These dipole couplings μ and d are in fact momentum-dependent form factors, and complex in general. They parameterize the effects arising at the loop level, which in principle could arise from both, interactions within the Standard Model (SM) and possible new interactions. If the measured values of the corresponding form factors deviate from the theoretical predictions of the conventional SM, this would indicate the presence of additional, new physics. Note that a possible experimental determination of non-vanishing $\mathrm{Im}(\mu)$ [$\mathrm{Im}(d\,)$] does not necessarily imply the existence of CP-conserving [CP-violating] new physics.

We use Eq. (1) to calculate the $t\bar{t}$ total cross section and the t and $\bar{t}$ polarizations to order $\alpha_s \equiv g_s^2/(4\pi)$. The extra diagrams contributing to this order are shown in Fig. 1, where the large dots represent anomalous couplings. The anomalous couplings enter in the amplitudes for soft and collinear gluon emissions. The infrared divergences in the amplitudes for soft gluon emission and in the virtual gluon corrections cancel as in standard QCD, since the anomalous terms vanish in the infrared limit. Moreover, we do not include anomalous couplings in the loop diagrams. The latter are included merely to regulate the infrared divergences. We thus study how anomalous couplings at tree-level would modify standard QCD predictions at order α_s.

For heavy-quark production, the standard QCD one-loop corrections to the total cross section and the longitudinal spin polarization [11] were calculated in closed analytic form before. Those results have been extended here to the case when anomalous couplings are present.

The total unpolarized production rate is given only in terms of the VV and AA parity-parity combinations for the Born contributions:

$$\sigma_{Born}\left(e^+e^- \to \gamma, Z \to q\bar{q}\right) = \tfrac{1}{2}v(3-v^2)\sigma^{VV} + v^3\sigma^{AA}, \tag{3}$$

where the mass parameters are $v = \sqrt{1-\xi}$ and $\xi = 4m_q^2/s$. The $O(\alpha_s)$ unpolarized case has the cross section

$$\sigma\left(e^+e^- \to \gamma, Z \to q\bar{q}\right) = \tfrac{1}{2}v(3-v^2)\sigma^{VV}c^{VV} + v^3\sigma^{AA}c^{AA}, \tag{4}$$

where the VV and AA factors that multiply with the appropriate Born terms are given below.

$$c^{VV} = 1 + \frac{\alpha_s}{2\pi}C_F\left[\tilde{\Gamma} - v\frac{\xi}{2+\xi}\ln\left(\frac{1+v}{1-v}\right) - \frac{4}{v}I_2 - \frac{\xi}{v}\tilde{I}_3 + \frac{4}{v(2+\xi)} + \frac{2-\xi}{v}\tilde{I}_5 + \Delta_0^{VV}\right]. \tag{5}$$

In this equation, the contribution from the virtual gluon loop is denoted as

$$\begin{aligned}\tilde{\Gamma} &= \left[2 - \frac{1+v^2}{v}\ln\left(\frac{1+v}{1-v}\right)\right]\ln\left(\tfrac{1}{4}\xi\right) + \frac{1+v^2}{v}\left[\mathrm{Li}_2\left(-\frac{2v}{1-v}\right) - \mathrm{Li}_2\left(\frac{2v}{1+v}\right) + \pi^2\right] \\ &\quad +3v\ln\left(\frac{1+v}{1-v}\right) - 4.\end{aligned} \tag{6}$$

Here, the $q\bar{q}g$ phase-space integrals are abbreviated by I_i, and $\tilde{I}_i$ specify the results after the (soft) IR divergences have canceled. The explicit analytical expressions for these phase-space integrals may be found in [12]. The additional component stemming from the anomalous gluon bremsstrahlung is given by

$$\Delta_0^{VV} = \frac{8}{(2+\xi)v}\left[\mathrm{Re}(\mu)(I_1+I_4) + \frac{2}{\xi}\left(|\mu|^2+|d|^2\right)(I_1-2I_8)\right]. \tag{7}$$

For the AA contribution we find:

$$c^{AA} = 1 + \frac{\alpha_s}{2\pi}C_F\left[\tilde{\Gamma} + 2\frac{\xi}{v}\ln\left(\frac{1+v}{1-v}\right) + \frac{\xi}{v^3}I_1 - \frac{4}{v}I_2 - \frac{\xi}{v}\tilde{I}_3 + \frac{2+\xi}{v^3}I_4 - \frac{2-\xi}{v}\tilde{I}_5 + \Delta_0^{AA}\right], \tag{8}$$

with the following anomalous part

$$\begin{aligned}\Delta_0^{AA} &= \frac{2}{v^3}\left[\mathrm{Re}(\mu)\Big\{-(4-\xi)I_1 + (2+\xi)I_4\Big\} + \left(|\mu|^2+|d|^2\right)\left\{\left(\frac{4}{\xi}+\xi-6\right)I_1 + \xi I_4\right.\right. \\ &\quad \left.\left. -\frac{4}{\xi}(2-\xi)I_8 + \frac{4}{\xi}I_9\right\}\right].\end{aligned} \tag{9}$$

The remaining VA and AV parts are identical and only contribute to the spin-dependent cross section. In the absence of anomalous couplings ($\mu = d = 0$), the cross section for

longitudinally polarized quarks of helicity $\pm\frac{1}{2}$ is given by

$$\sigma\left(e^+e^-\to\gamma,Z\to q(\lambda_\pm)\,\bar{q}\right)=\tfrac{1}{2}v(3-v^2)\sigma^{VV}c^{VV}+v^3\sigma^{AA}c^{AA}\pm v^2\sigma_S^{VA}c_\pm^{VA}. \tag{10}$$

The multiplication factors c^{ij} are expressed in terms of phase-space integrals of type S_i:

$$c_\pm^{VA,AV}=1+\frac{\alpha_s}{2\pi}C_F\left[\tilde{\Gamma}+\frac{\xi}{v}\ln\left(\frac{1+v}{1-v}\right)+\Delta_{\mu=d=0}^{VA,AV}\right], \tag{11}$$

where

$$\begin{aligned}\Delta_{\mu=d=0}^{VA,AV} &= \tfrac{1}{2}\Big[(4-\xi)S_1-(4-5\xi)S_2-2(4-3\xi)S_4-\xi(1-\xi)(\tilde{S}_3+\tilde{S}_5)+\xi(S_6-S_7)\\ &\quad -2S_8+(2-\xi)S_9+(6-\xi)S_{10}-2S_{11}+2(1-\xi)(2-\xi)S_{12}\Big].\end{aligned} \tag{12}$$

The full analytic forms of all relevant S integrals are too lengthy to be exhibited here. Most of them are compiled in Ref. [12], except for the four additional integrals S_{14}, S_{15}, S_{16}, and S_{17}, which are discussed in more detail in the appendix.

Including spins for the quark or the antiquark introduces additional spin-flip terms in the $O(\alpha_s)$ c factors given in Eqs. (5), (8) and (11). For longitudinal quark polarization we find

$$c_\pm^{ij}=\tfrac{1}{2}\left[c^{ij}\pm\frac{\alpha_s}{2\pi}C_F\Delta_S^{ij}\right]. \tag{13}$$

The individual parity-parity combinations are

$$\begin{aligned}(2+\xi)v\,\Delta_S^{VV} &= 8\,\mathrm{Im}\,(\mu^*d)\left[-2\left(1-\frac{2}{\xi}\right)S_1+\left(1-\frac{4}{\xi}\right)S_8-S_9-S_{10}+S_{11}\right.\\ &\qquad \left.+2\left(1-\frac{4}{\xi}\right)S_{13}+\frac{4}{\xi}(S_{15}+S_{17})\right]\\ &\quad +\mathrm{Im}(d)\Big[8(1-\xi)S_1-\Big\{8-3\xi(2-\xi)\Big\}S_2+\Big\{8+\xi(2-3\xi)\Big\}S_4\\ &\qquad -\xi(2+\xi)S_6-4S_8+4(1-\xi)S_9-4(3+\xi)S_{10}+4S_{11}\\ &\qquad +\xi(2-\xi)S_{14}\Big],\end{aligned} \tag{14}$$

$$\begin{aligned}v^3\Delta_S^{AA} &= 4\,\mathrm{Im}\,(\mu^*d)\left[\frac{2}{\xi}(1-\xi)(2-\xi)S_1+\left(5-\frac{4}{\xi}\right)S_8-(1-\xi)(S_9+S_{10})+S_{11}\right.\\ &\qquad \left.+2\left(3-\frac{4}{\xi}\right)S_{13}-2\left(1-\frac{2}{\xi}\right)S_{15}-\frac{4}{\xi}S_{16}-2\left(1-\frac{4}{\xi}\right)S_{17}\right]\end{aligned}$$

$$+\,\mathrm{Im}(d)\Big[\,2\xi S_1-(1-\xi)(4-\xi)(S_2-S_4)-\xi(1-\xi)S_6-(2-\xi)S_8$$
$$+(2-3\xi)S_9-(6-5\xi)S_{10}+(2+\xi)(S_{11}+2S_{13})+\xi(1-\xi)S_{14}\Big], \quad (15)$$

$$\begin{aligned} v^2\Delta_S^{VA,AV} &= \mathrm{Re}(\mu)\Big[\,-\xi(S_1+S_7)-2S_8+(2-\xi)(S_9+S_{10})-2S_{11}\,\Big] \\ &\pm 2\,i\,\mathrm{Im}(\mu)\Big[\,(2-\xi)S_1-\xi S_{10}-2S_{13}\,\Big] \qquad (16) \\ &+\Big(|\mu|^2+|d|^2\Big)\Big[\,-(4-\xi)S_1-\xi S_7+4S_8+\xi S_9+(4-\xi)S_{10}-4S_{11}\,\Big]. \end{aligned}$$

Using charge conjugation in the final state, one can readily obtain the corresponding expressions for (longitudinal) antiquark polarization. In the following, we denote the antiquark results by an additional bar, *i.e.* $\bar{\Delta}_S^{ij}$:

$$\bar{\Delta}_S^{VV} = \Delta_S^{VV}, \quad (17)$$
$$\bar{\Delta}_S^{AA} = \Delta_S^{AA}, \quad (18)$$

where the following identities hold

$$\bar{\Delta}^{VA} = -\Delta_S^{VA} = \Big(\bar{\Delta}_S^{AV}\Big)^*, \quad (19)$$
$$\text{with} \qquad \bar{\Delta}_S^{AV} = -\Delta_S^{AV}. \quad (20)$$

Considering the above expressions, we can construct the following combinations of polarization asymmetries of t and $\overline{t}$,

$$\Delta\sigma^{(+)} = \tfrac{1}{2}\Big[\,\sigma(\uparrow)-\sigma(\downarrow)-\overline{\sigma}(\uparrow)+\overline{\sigma}(\downarrow)\,\Big], \quad (21)$$

$$\Delta\sigma^{(-)} = \tfrac{1}{2}\Big[\,\sigma(\uparrow)-\sigma(\downarrow)+\overline{\sigma}(\uparrow)-\overline{\sigma}(\downarrow)\,\Big], \quad (22)$$

where $\sigma(\uparrow)$, $\overline{\sigma}(\uparrow)$ refer respectively to the cross sections for top and antitop with positive helicity, and $\sigma(\downarrow)$, $\overline{\sigma}(\downarrow)$ are the same quantities with negative helicity. Of these, $\Delta\sigma^{(+)}$ is CP even and $\Delta\sigma^{(-)}$ is CP odd. This is obvious from the fact that under C, σ and $\overline{\sigma}$ get interchanged, while under P, the helicities of both t and $\overline{t}$ get flipped. Consequently, σ and $\Delta\sigma^{(+)}$, both nonzero in standard QCD, receive contributions from combinations of

anomalous couplings which are CP even, viz., $\mathrm{Im}(\mu)^2+|d|^2$ and $\mathrm{Re}(\mu)$. On the other hand, $\Delta\sigma^{(-)}$ vanishes in standard QCD, and in the presence of anomalous couplings it depends only on the CP-odd variables $\mathrm{Im}(\mu^* d)$ and $\mathrm{Im}(d)$. That $\Delta\sigma^{(-)}$ depends on the imaginary parts rather than the real parts of a combination of couplings follows from the fact that it is even under naive time reversal $\mathrm{T_N}$, i.e., reversal of all momenta, without change in helicities, and without interchange of initial and final states (as would have been required by genuine time reversal). As a consequence, it is odd under $\mathrm{CPT_N}$, and imaginary parts of couplings have to appear in order to avoid conflict with the CPT theorem.

3 Numerical results

Figs. 2a and 2b show the dependence of $\Delta\sigma^{(+)}$ on $\sqrt{\mathrm{Im}(\mu)^2+|d|^2}$ and $\mathrm{Re}(\mu)$ at $\sqrt{s}=500$ GeV and 1000 GeV, respectively. Figs. 3a and 3b depict $\Delta\sigma^{(-)}$ plotted against $\mathrm{Im}(\mu^* d)$ and $\mathrm{Im}(d)$.

We would now like to see how sensitive experiments at a future linear collider would be to the anomalous quantities μ and d. Since these are determined through $\Delta\sigma^{(+)}$ and $\Delta\sigma^{(-)}$, we should know how well these latter quantities can be measured experimentally. The quantity $\sigma(\uparrow)-\sigma(\downarrow)$ is simply the polarization P_t of the top quark in the production process, and it can be determined by looking at the angular distribution of the decay products of the top. For example, in the decay mode $t\to W^+b$, the angular distribution of the b quark in the t quark rest frame is

$$\frac{1}{\Gamma}\frac{d\Gamma}{d\Omega_b}=\frac{1}{4\pi}\Big(1+P_t\,\alpha\,\hat{p}_b\cdot\vec{s}\Big), \tag{23}$$

where $\vec{p}_b$ is the b-quark momentum and $\vec{s}$ is the top spin. This angular distribution can be used to determine P_t. In Eq. (23), the parameter α ($|\alpha|\le 1$) is a constant known as the *analyzing power* for the decay channel. In this particular case, α is given by

$$\alpha=\frac{m_t^2-2m_W^2}{m_t^2+2m_W^2}\ . \tag{24}$$

There is an analogous expression for the decay $\overline{t} \to W^- \overline{b}$. If the angular distribution of a lepton or a jet arising from W decay is used to determine P_t, the corresponding analyzing power would be different. The efficiency with which the top or antitop polarization can be measured will depend not only on the analyzing power of the channel, but also on the detection efficiency of the observed particles, like the b quark. While the tagging efficiency of the b would be much better at e^+e^- colliders than at hadron colliders, because of the lower hadronic activity, it would nevertheless depend on the degree to which backgrounds are understood and eliminated. A more detailed analysis in the context of specific experimental conditions would be needed to obtain the overall top polarization detection efficiency, which we parameterize as ϵ in what follows.

We use our expressions to obtain simultaneous 90% confidence level (CL) limits that could be obtained at a future linear collider with an integrated luminosity of 50 fb^{-1}. We do this by equating the magnitude of the difference between the values for a quantity with and without anomalous couplings to 2.15 times the statistical error expected. Thus, the limiting values of $\mathrm{Im}(\mu)^2 + |d|^2$ and $\mathrm{Re}(\mu)$ for an integrated luminosity L and a top detection efficiency of ϵ are obtained from

$$\epsilon\, L\, |\, \sigma(\mu, d) - \sigma_{SM}\, | = 2.15\, \sqrt{L\, \sigma_{SM}} \tag{25}$$

and

$$\epsilon\, L\, \left|\, \Delta\sigma^{(+)}(\mu, d) - \Delta\sigma^{(+)}_{SM}\, \right| = 2.15\, \sqrt{L\, |\, \sigma_{SM}(\uparrow) - \overline{\sigma}_{SM}(\uparrow)\, |}\,, \tag{26}$$

whereas the limiting values of $\mathrm{Im}(\mu^* d)$ and $\mathrm{Im}(d)$ are obtained from

$$\epsilon\, L\, \left|\, \Delta\sigma^{(-)}(\mu, d) - \Delta\sigma^{(-)}_{SM}\, \right| = 2.15\, \sqrt{L\, |\, \sigma_{SM}(\uparrow) + \overline{\sigma}_{SM}(\uparrow)\, |}\,. \tag{27}$$

In the above expressions, the subscript "SM" denotes the value expected in the standard model, with $\mu = d = 0$. We use $L = 50$ fb^{-1} and $\epsilon = 0.1$ in our numerical estimates. The value of ϵ depends on the details of the detector, as well as the kinematical cuts employed. The value we use is only representative, and it would be easy to obtain limits for any other value of ϵ by appropriate scaling, because of the simple dependence on ϵ in Eqs. (25), (27), and (26).

For the running of the strong coupling, we choose $\alpha_s^{(5)}(M_Z) = 0.118$ (with $M_Z = 91.178$ GeV) in the modified minimal subtraction scheme and use the appropriate conditions to match for six active flavours[2].

Eqs. (25) and (26) are used to obtain contours in the plane of $\sqrt{\mathrm{Im}(\mu)^2 + |d|^2}$ and $\mathrm{Re}(\mu)$. The contours from (25) are shown in Figs. 4a and 4b for $\sqrt{s} = 500$ GeV and 1000 GeV, respectively. The contours obtained from (26) are shown in Figs. 5a and 5b. Eq. (27) gives contours in the plane of $\mathrm{Im}(\mu^* d)$ and $\mathrm{Im}(d)$, which are displayed in Figs. 6a and 6b. For different e^- longitudinal beam polarizations P_-, the corresponding contours are presented in Figs. 4–6. In Figs. 4 and 5, the allowed regions are the ones shown below the respective contours. In Figs. 6a,b, the allowed regions are bands lying between the upper and lower straight lines.

In principle, the measurement of two independent quantities σ and $\Delta\sigma^{(+)}$ could have given independent limits on $\mathrm{Im}(\mu)^2 + |d|^2$ and $\mathrm{Re}(\mu)$. However, a comparison of Figs. 4 and 5 shows that this possibility is not realized. A superposition of Figs. 4a,b and 5a,b is shown in Fig. 7a. It can be seen that the allowed region coming from σ lies entirely within the allowed region from $\Delta\sigma^{(+)}$, with no intersection between the two. Thus σ is more sensitive to the anomalous CP-even couplings as compared to $\Delta\sigma^{(+)}$. Moreover, each contour for $\sqrt{s} = 1000$ GeV lies within the corresponding contour for $\sqrt{s} = 500$ GeV, showing a uniform increase in sensitivity with c.m. energy.

The other conclusion that can be drawn from Figs. 4 and 5 is that a large left-handed polarization leads to increase in sensitivity.

The best limits obtainable from σ at $\sqrt{s} = 500$ GeV are $-3 < \mathrm{Re}(\mu) < 2$ for $\mathrm{Im}(\mu) = 0 = d$, and $\sqrt{\mathrm{Im}(\mu)^2 + |d|^2} < 2.25$ for $\mathrm{Re}(\mu) = 0$. These limits are improved by about a factor 2 in going to $\sqrt{s} = 1000$ GeV for the same integrated luminosity.

In the case of CP-odd combinations of the couplings $\mathrm{Im}(\mu^* d)$ and $\mathrm{Im}(d)$, there is only one

[2]It is common to indicate the number of active flavours as superscript of α_s. For practical purposes one usually selects bottom production as reference. Here, our choice for $\alpha_s^{(5)}(M_Z)$ translates to $\alpha_s^{(6)}(M_t = 172.1\mathrm{GeV}) = 0.10811$

measurable CP-odd quantity $\Delta\sigma^{(-)}$ at each c.m. energy, and therefore independent limits on the two combinations are not possible. Fig. 6a shows that for $\sqrt{s} = 500$ GeV, the best limits which can be obtained are for $P = -1$, viz., $-3.6 < \mathrm{Im}(\mu^* d) < 3.6$ for $\mathrm{Im}(d) = 0$ and $-10 < \mathrm{Im}(d) < 10$ for $\mathrm{Im}(\mu^* d) = 0$. The corresponding limits for $\sqrt{s} = 1000$ GeV, as seen from Fig. 6b, are $-0.4 < \mathrm{Im}(\mu^* d) < 0.4$ for $\mathrm{Im}(d) = 0$ and $-20 < \mathrm{Im}(d) < 20$ for $\mathrm{Im}(\mu^* d) = 0$. However, if a measurement of $\Delta\sigma^{(-)}$ is made at two c.m. energies, a relatively narrow allowed range can be obtained, allowing *independent* limits to be placed on both $\mathrm{Im}(\mu^* d)$ and $\mathrm{Im}(d)$. This is demonstrated in Fig. 7b. In fact, the improvement in the limit on $\mathrm{Im}(\mu^* d)$ in going from $\sqrt{s} = 500$ GeV to $\sqrt{s} = 1000$ GeV is considerable. The possible limits are

$$-0.8 < \mathrm{Im}(\mu^* d) < 0.8, -11 < \mathrm{Im}(d) < 11. \tag{28}$$

These limits may be compared with the limits obtainable from gluon jet energy distribution in $e^+e^- \to t\bar{t}g$ [4]. While our proposal for the CP-even case seems to fare worse, for the CP-odd case, our proposal can be competitive. It should however be emphasized that in the case of the CP-odd couplings, we are proposing the measurement of a genuinely CP-violating quantity, whereas the analysis in [4] is merely based on the energy spectrum resulting from both CP-odd and CP-even couplings. In case of $\Delta\sigma^{(-)}$, the dependence on e^- beam polarization is rather mild.

4 Conclusions

It is worthwhile noting that we have used a rather conservative value of $\epsilon = 0.1$ for top detection and polarization analysis. A better efficiency would lead to an improvement in the limits, as would a higher luminosity.

We have not considered the effect of initial-state radiation in this work. We have also ignored possible effects of collinear gluon emission from one of the decay products of t or $\bar{t}$. A complete analysis should indeed incorporate these effects, as well as a study of t and

$\overline{t}$ decay distributions which can be used to measure the polarizations. However, we do not expect our conclusions to change drastically when these effects are taken into account.

In summary, we have examined the capability of total cross section and single quark polarization in $e^+e^- \to t\overline{t}$ to measure or put limits on anomalous chromomagnetic and chromoelectric dipole couplings. While the total cross section measurements can give, for the luminosities assumed, limits of order 1 on the CP-even couplings, only the CP-violating combination of top and antitop polarizations is sensitive to anomalous couplings, and can yield a limit of the order of 1 on a CP-odd combination of anomalous couplings.

Acknowledgments. We are both grateful for the kind hospitality and stimulating scientific atmosphere we enjoyed at the Departament de Fí sica Teòrica during the principal stages of this work. We thank Bar-Shalom Shaouly for pointing out the update of Figures 6. This work has been supported by the DGICYT under Grants Ns. PB95-1077 and SAB95-0175, as well as by the TMR network ERBFMRXCT960090 of the European Union (S.D.R.). M.M.T. acknowledges support by CICYT Grant AEN-96/1718 and the Max-Kade Foundation, New York, NY.

Appendix: Additional Phase-Space Integrals

The complicated three-body phase-space for the process $e^+e^- \to q(\uparrow)\bar{q}g$ is best solved analytically by using the kinematic variables $y = 1 - p_1 \cdot q/q^2$ and $z = 1 - p_2 \cdot q/q^2$, which are natural dimensionless parameters referring to the quark and antiquark energies (including the radiated gluon) in the centre-of-mass system. Then, the relevant phase-space integrands all result in simple rational functions containing polynomials in y and z, and the corresponding integration boundary is described by the symmetric solution of a (y, z)-biquadratic form [11, 12].

Apart from the detailed integral list of Ref. [12], in this particular calculation four new integrals emerged. For completeness, we give here the following full analytical results:

$$\begin{aligned} S_{14} &= \int \frac{dy\,dz}{\sqrt{(1-y)^2-\xi}}\ \frac{z}{y^2} \\ &= \frac{2}{\xi} - \frac{2+\sqrt{\xi}}{2(2-\sqrt{\xi})} - \ln(2-\sqrt{\xi}) + \tfrac{1}{2}\ln\xi - \tfrac{1}{2}, \end{aligned} \tag{A.1}$$

$$\begin{aligned} S_{15} &= \int \frac{dy\,dz}{\sqrt{(1-y)^2-\xi}}\ y^2 \\ &= \tfrac{1}{32}\xi^3\Big[\tfrac{1}{2}\ln\xi - \ln(2-\sqrt{\xi})\Big] - \sqrt{\xi}\left(4 + \tfrac{1}{3}\xi + \tfrac{1}{4}\xi^2\right) \\ &\quad + \tfrac{1}{8}\left(7 - \tfrac{1}{2}\xi\right)\xi + \tfrac{1}{3}, \end{aligned} \tag{A.2}$$

$$\begin{aligned} S_{16} &= \int \frac{dy\,dz}{\sqrt{(1-y)^2-\xi}}\ y^2 z \\ &= -\frac{\xi^4(4-\xi)}{512(2-\sqrt{\xi})^2} + \tfrac{1}{16}\left(\tfrac{3}{16}\xi - 1\right)\ln(2-\sqrt{\xi}) - \tfrac{3}{8}\xi\left(1 + \tfrac{3}{8}\xi\right) \\ &\quad + \tfrac{1}{512}\xi^3\Big[4 - \xi + (16-3\xi)\ln\xi\Big] + \tfrac{1}{4}\left(\tfrac{7}{3} - \tfrac{1}{2}\xi + \tfrac{1}{16}\xi^2\right) + \tfrac{1}{24}, \end{aligned} \tag{A.3}$$

$$S_{17} = \int \frac{dy\,dz}{\sqrt{(1-y)^2-\xi}}\ y\,z$$

$$
\begin{aligned}
= \;& \tfrac{1}{32}\xi^2(6-\xi)\Big[-\tfrac{1}{2}\ln\xi+\ln(2-\sqrt{\xi})\Big]+\tfrac{1}{128}(4-\xi)\frac{\xi^3}{(2-\sqrt{\xi})^2} \\
& +\tfrac{1}{4}\xi^{\frac{3}{2}}\left(\tfrac{5}{3}-\tfrac{1}{8}\xi\right)-\tfrac{1}{2}\xi\left(1-\tfrac{1}{64}\xi^2\right)+\tfrac{1}{12}, \qquad \text{(A.4)}
\end{aligned}
$$

where the usual mass parameters are $v=\sqrt{1-\xi}$ and $\xi=4m_q^2/s$.

Note that there are no soft divergences in these particular integrals. The collinear divergences contained in these integrals arise from the massless character of the fermion field, and are easily identified by observing the limit $\xi \to 0$. In our full analytical expressions for the polarized cross sections with VV and AA parity-parity combinations, integral S_{14} is multiplied by the mass factor ξ, viz. Eqs. (14) and (15). This produces additional finite contributions, which originate from a collinear helicity-flip with anomalous chromoelectric couplings, and are absent in a naive massless model.

References

[1] P. Tipton, CDF collaboration, plenary talk at the *28th International Conference on High Energy Physics*, Warsaw, July 1996.

[2] S.D. Rindani, Pramana - J. Phys. Suppl. **45** (1995) 263; D. Atwood and A. Soni, BNL-THY-AS-9-1996, 1996, Proceedings of 28th International Conference on High-energy Physics (ICHEP 96), Warsaw, (to appear), BNL-THY-AS-9-1996, hep-ph/9609418; W. Bernreuther, Aachen preprint PITHA 97/3 (1997), hep-ph/9701357; P. Poulose and S.D. Rindani, Phys. Rev. **D57** (1998) 5444, hep-ph/9709225.

[3] J.P. Ma and A. Brandenburg, Z. Phys. **C56** (1992) 97; A. Brandenburg and J.P. Ma, Phys. Lett. **B298** (1993) 211. D. Atwood, A. Aeppli and A. Soni, Phys. Rev. Lett. **69** (1992) 2754; P. Haberl, O. Nachtmann and A. Wilch, Phys. Rev. **D53** (1996) 4875; T.G. Rizzo, Stanford report SLAC-PUB-7294 (1996), hep-ph/9609311; K. Cheung, Phys. Rev. **D53** (1996) 3604, Phys. Rev. **D55** (1997) 4430, hep-ph/9610368 (1996);

[4] T.G. Rizzo, Stanford report, SLAC-PUB-7317 (1996), hep-ph/9610373.

[5] S. Parke and Y. Shadmi, Phys. Lett. **B387** (1996) 199, hep-ph/9606419.

[6] C.T. Hill and S.J. Parke, Phys. Rev. **D49** (1994) 4454, hep-ph/9312324.

[7] B. Grzadkowski and Z. Hioki, Probing CP violation via top polarization at NLC, hep-ph/9610306; Probing top-quark couplings at polarized NLC, hep-ph/9805318.

[8] C.P. Yuan, Phys. Rev. **D45** (1992) 782.

[9] I. Bigi and H. Krasemann, Z. Phys. **C7** (1981) 127; J. Kühn, Acta Phys. Austr. Suppl. **XXIV** (1982) 203; I. Bigi et al., Phys. Lett. **B181** (1986) 157.

[10] Saurabh D. Rindani and Michael M. Tung, Phys. Lett. **B424** (1998) 125, hep-ph/9702349.

[11] J.G. Körner, A. Pilaftsis and M.M. Tung, Z. Phys. **C63** (1994) 575; M.M. Tung, Ph.D. thesis, University of Mainz (1993), and Phys. Rev. **D52** (1995) 1353, hep-ph/9403322.

[12] M.M. Tung, J. Bernabéu, J. Peñarrocha, Nucl. Phys. **B470** (1996) 41, hep-ph/9601277.

Figure Captions

Fig. 1: Additional Feynman diagrams contributing to $\sigma\left(e^+e^- \to \gamma, Z \to t\bar{t}\right)$ that account for anomalous gluon couplings at $O(\alpha_s)$. The large dots represent anomalous $t\bar{t}g$ insertions according to the effective action Eq. (1).

Fig. 2: Surface plots displaying the dependence of the polarization asymmetry $\Delta\sigma^{(+)}$ on $\sqrt{\mathrm{Im}(\mu)^2 + |d|^2}$ and $\mathrm{Re}(\mu)$ with initial electron beam polarization $P_- = -1$ and c.m. energies **(a)** $\sqrt{s} = 500$ GeV, **(b)** $\sqrt{s} = 1000$ GeV.

Fig. 3: $\Delta\sigma^{(-)}$ surface plots showing the linear dependence on $\mathrm{Im}(\mu^* d)$ and $\mathrm{Im}(d)$ for **(a)** $\sqrt{s} = 500$ GeV and **(b)** $\sqrt{s} = 1000$ GeV with longitudinal beam polarization $P_- = -1$.

Fig. 4: Contour plots showing the allowed regions for σ_{SM} with 90% confidence level (integrated luminosity $L = 50$ fb^{-1} and top detection efficiency $\epsilon = 0.1$). Representative c.m. energies are **(a)** $\sqrt{s} = 500$ GeV and **(b)** $\sqrt{s} = 1000$ GeV for various longitudinal electron polarizations.

Fig. 5: $\Delta\sigma^{(+)}$ contour plots with 90% confidence level at c.m. energies: **(a)** $\sqrt{s} = 500$ GeV and **(b)** $\sqrt{s} = 1000$ GeV.

Fig. 6: $\Delta\sigma^{(-)}$ contour plots with 90% confidence level at c.m. energies: **(a)** $\sqrt{s} = 500$ GeV and **(b)** $\sqrt{s} = 1000$ GeV.

Fig. 7: **(a)** Superposition of Figs. 4 and 5, displaying combined allowed regions for both σ_{SM} and $\Delta\sigma^{(+)}$ polarization asymmetries. **(b)** Intersecting area resulting from two independent $\Delta\sigma^{(-)}$ measurements at $\sqrt{s} = 500$ GeV, 1000 GeV.

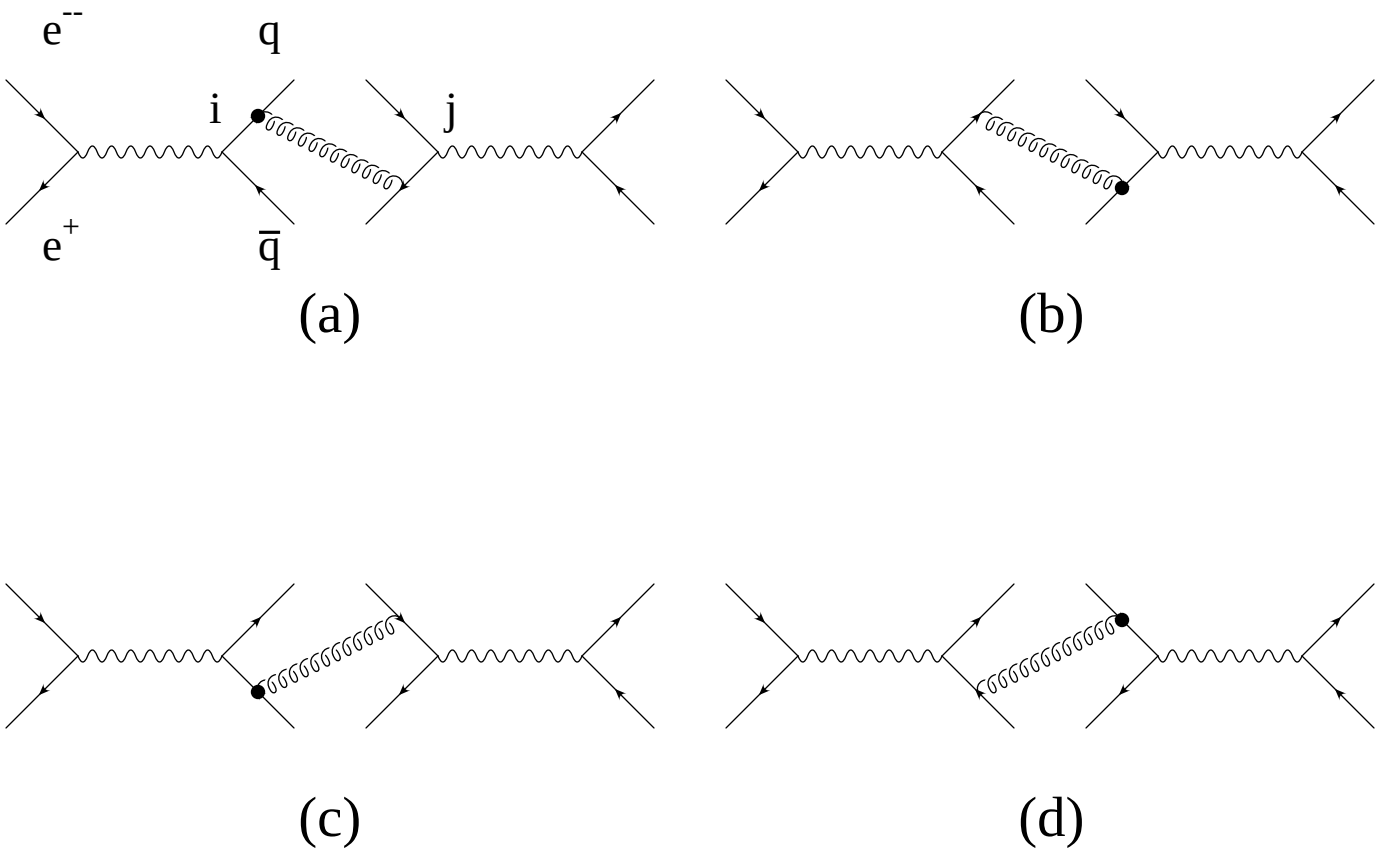

Figure 1

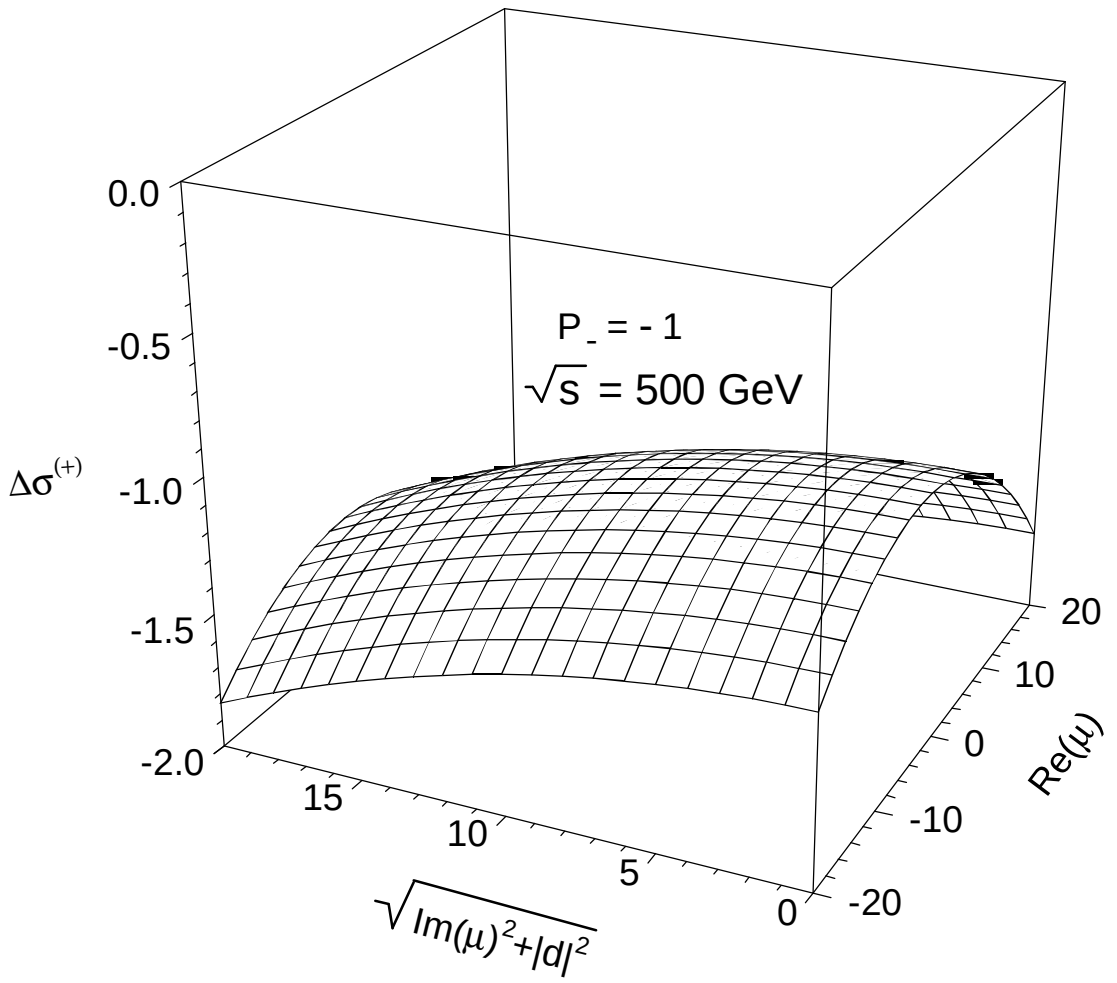
0.0
-0.5
-1.0
-1.5
-2.0
$\Delta\sigma^{(+)}$
$P_- = -1$
$\sqrt{s}$ = 500 GeV
15
10
5
0
$\sqrt{Im(\mu)^2+|d|^2}$
20
10
0
-10
-20
$Re(\mu)$

Figure 2a

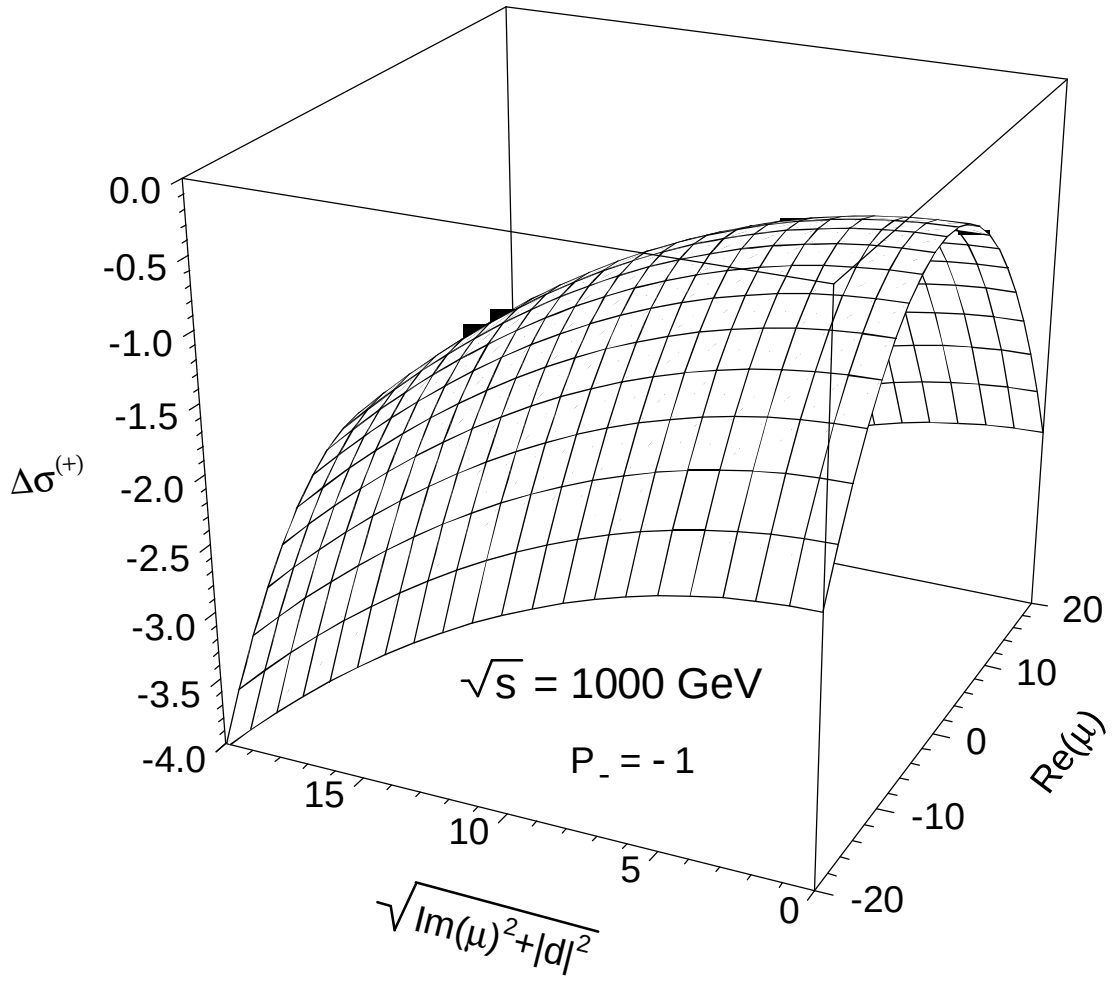
0.0
-0.5
-1.0
-1.5
-2.0
-2.5
-3.0
-3.5
-4.0
Δσ(+)
√s = 1000 GeV
P_ = - 1
15
10
5
0
√Im(μ)²+|d|²
20
10
0
-10
-20
Re(μ)

Figure 2b

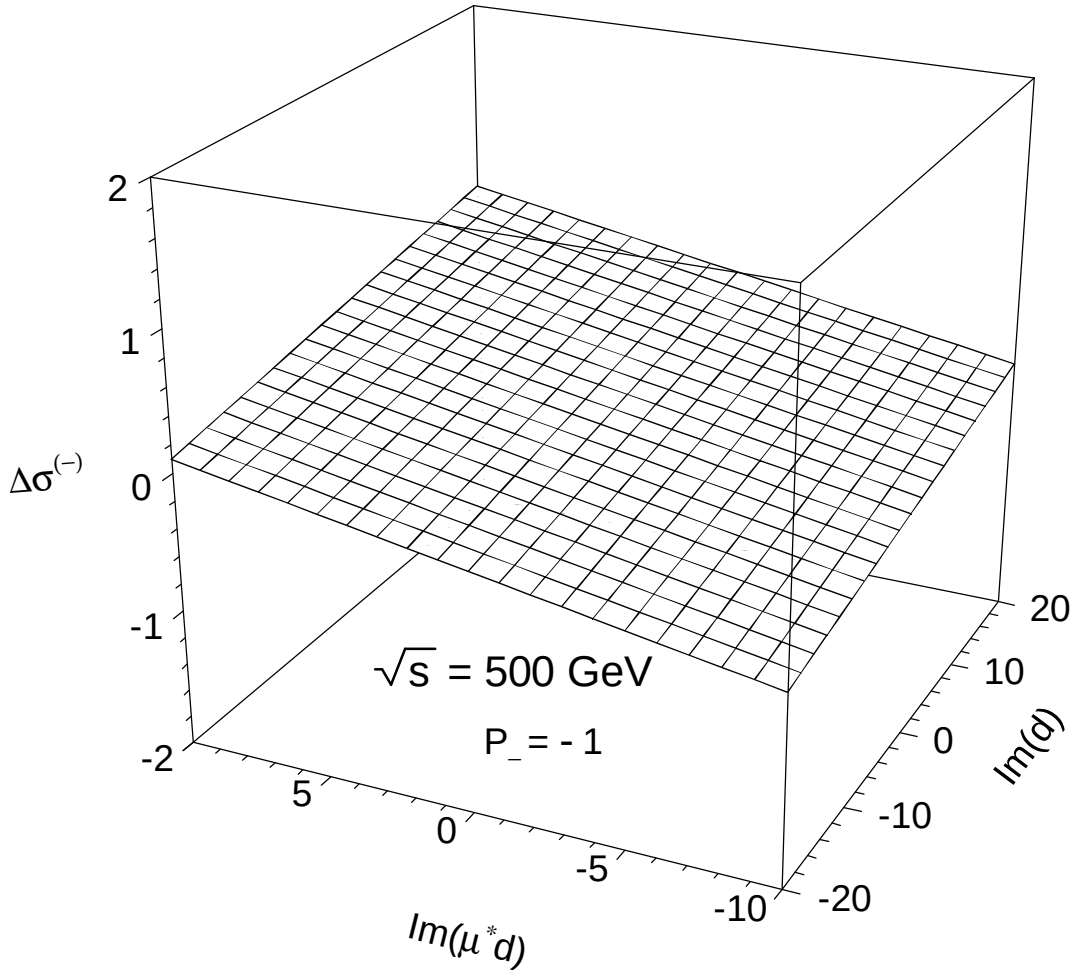

Figure 3a

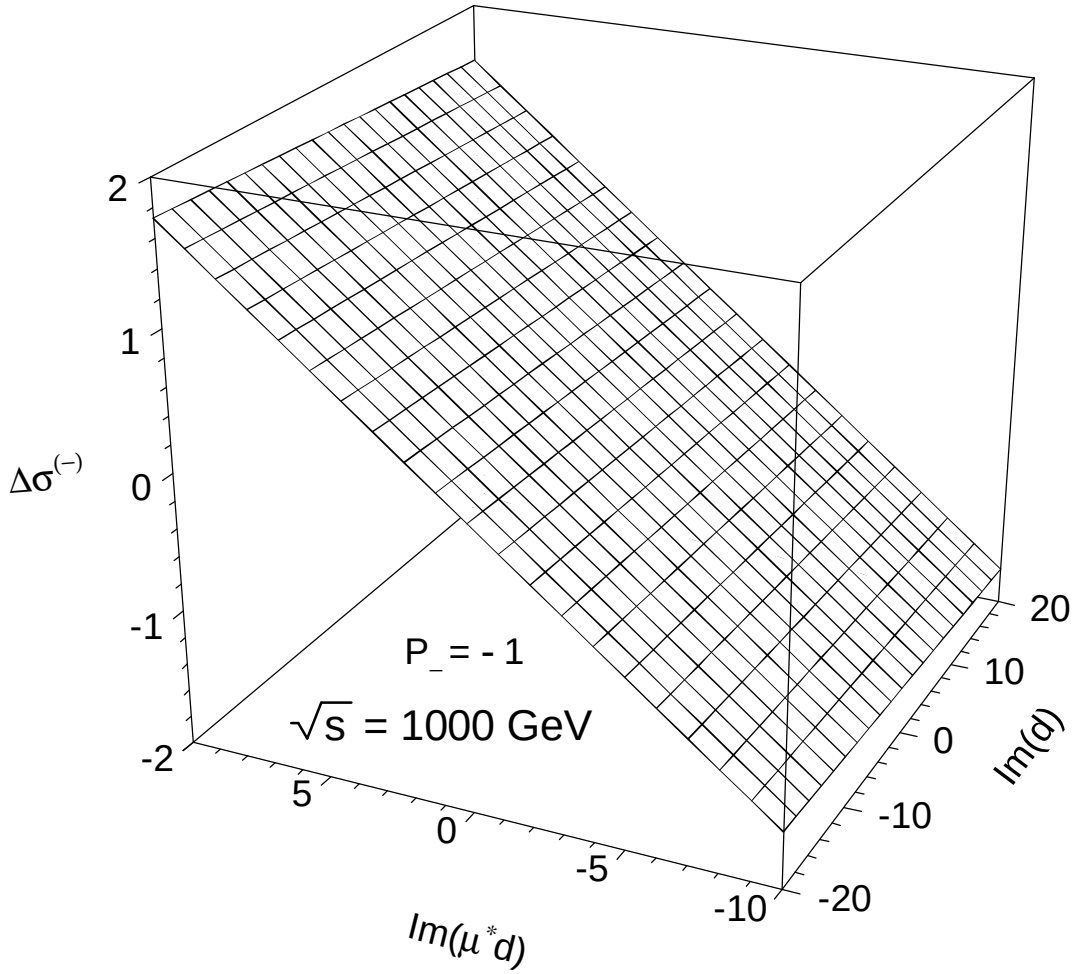

Figure 3b

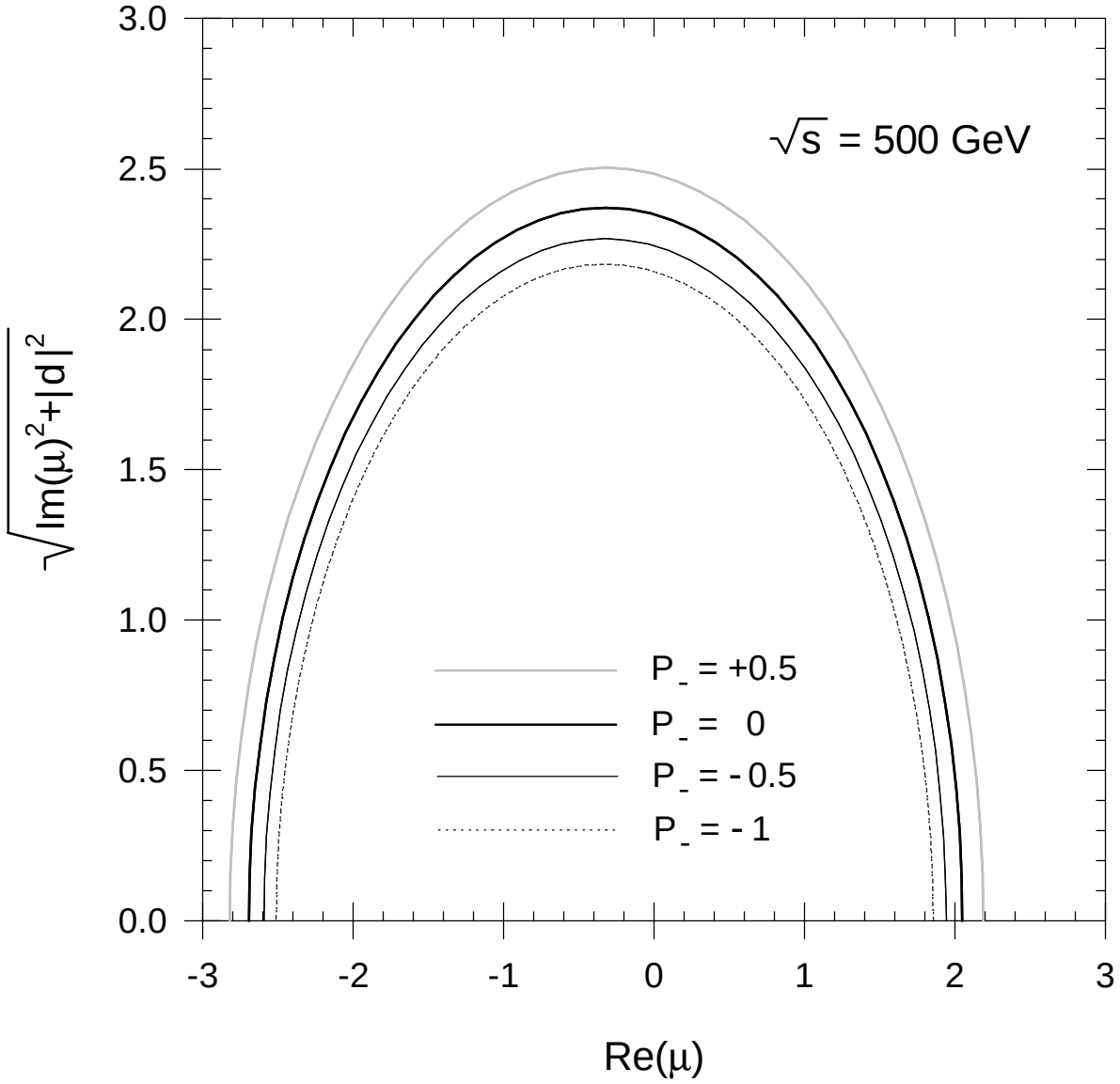

Figure 4a

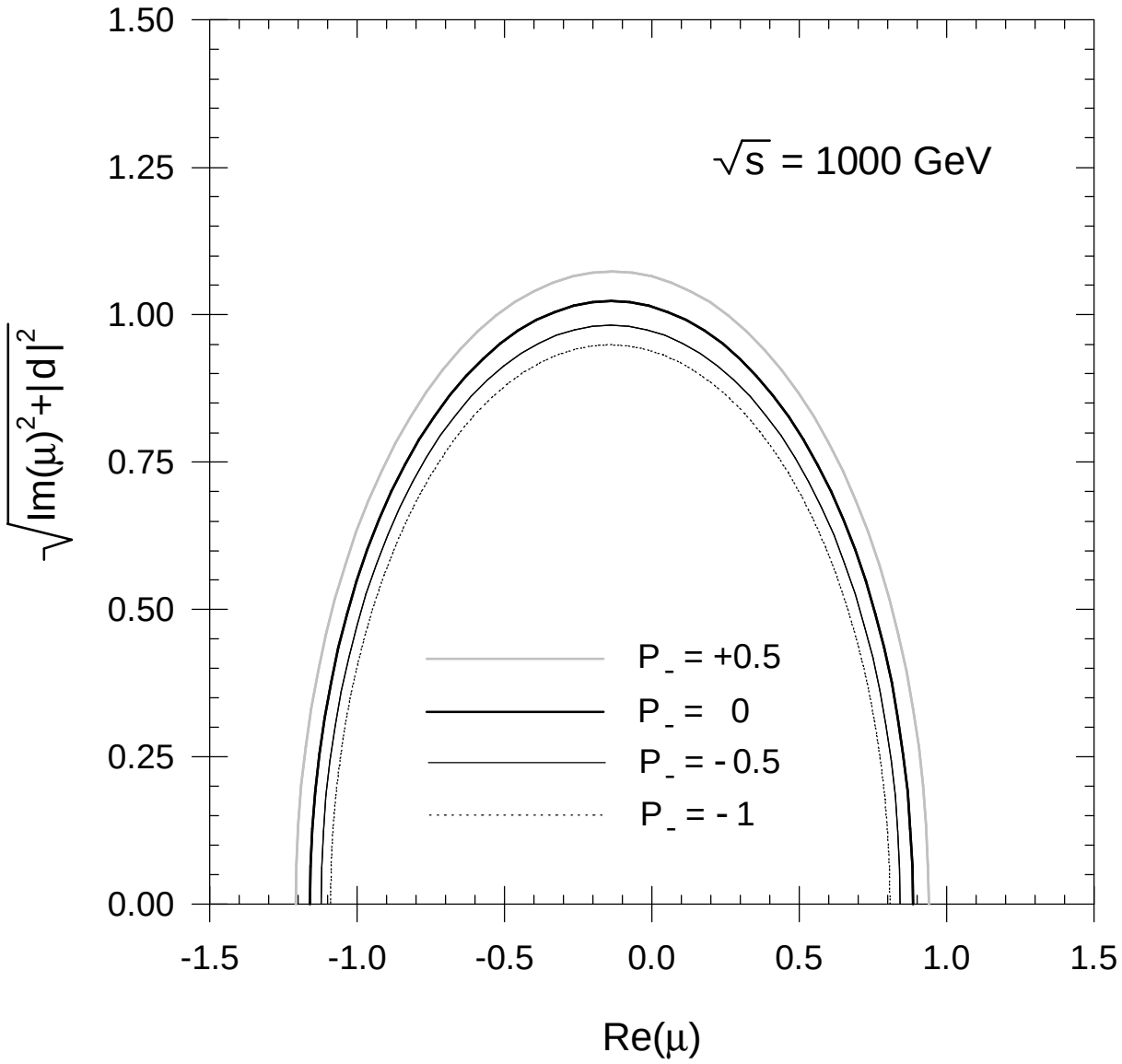
1.50
1.25
1.00
0.75
0.50
0.25
0.00
-1.5
-1.0
-0.5
0.0
0.5
1.0
1.5
√s = 1000 GeV
P_ = +0.5
P_ = 0
P_ = - 0.5
P_ = - 1
√Im(μ)²+|d|²
Re(μ)

Figure 4b

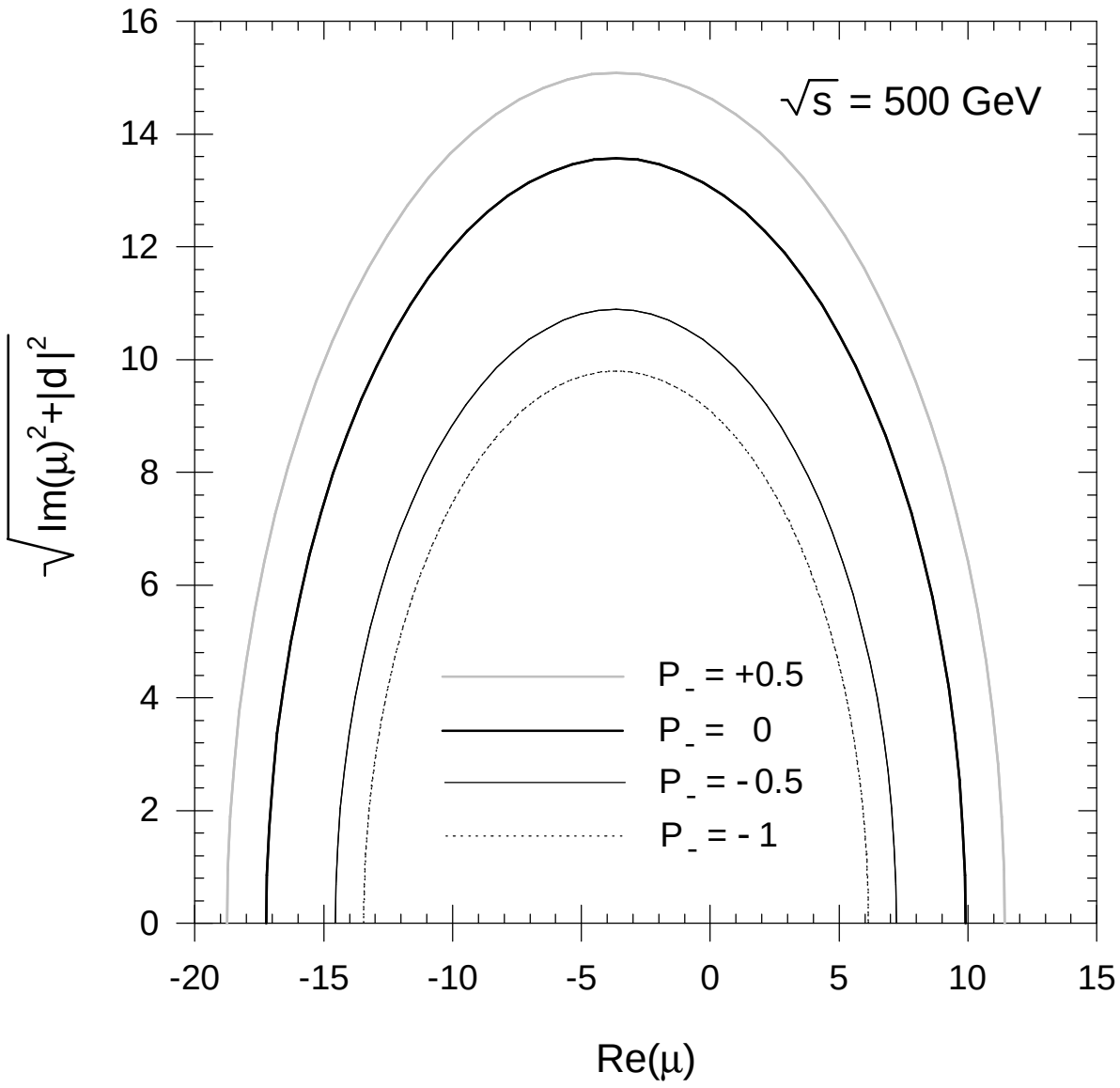
16
14
12
10
8
6
4
2
0
-20
-15
-10
-5
0
5
10
15
√s = 500 GeV
P_ = +0.5
P_ = 0
P_ = - 0.5
P_ = - 1
√Im(μ)²+|d|²
Re(μ)

Figure 5a

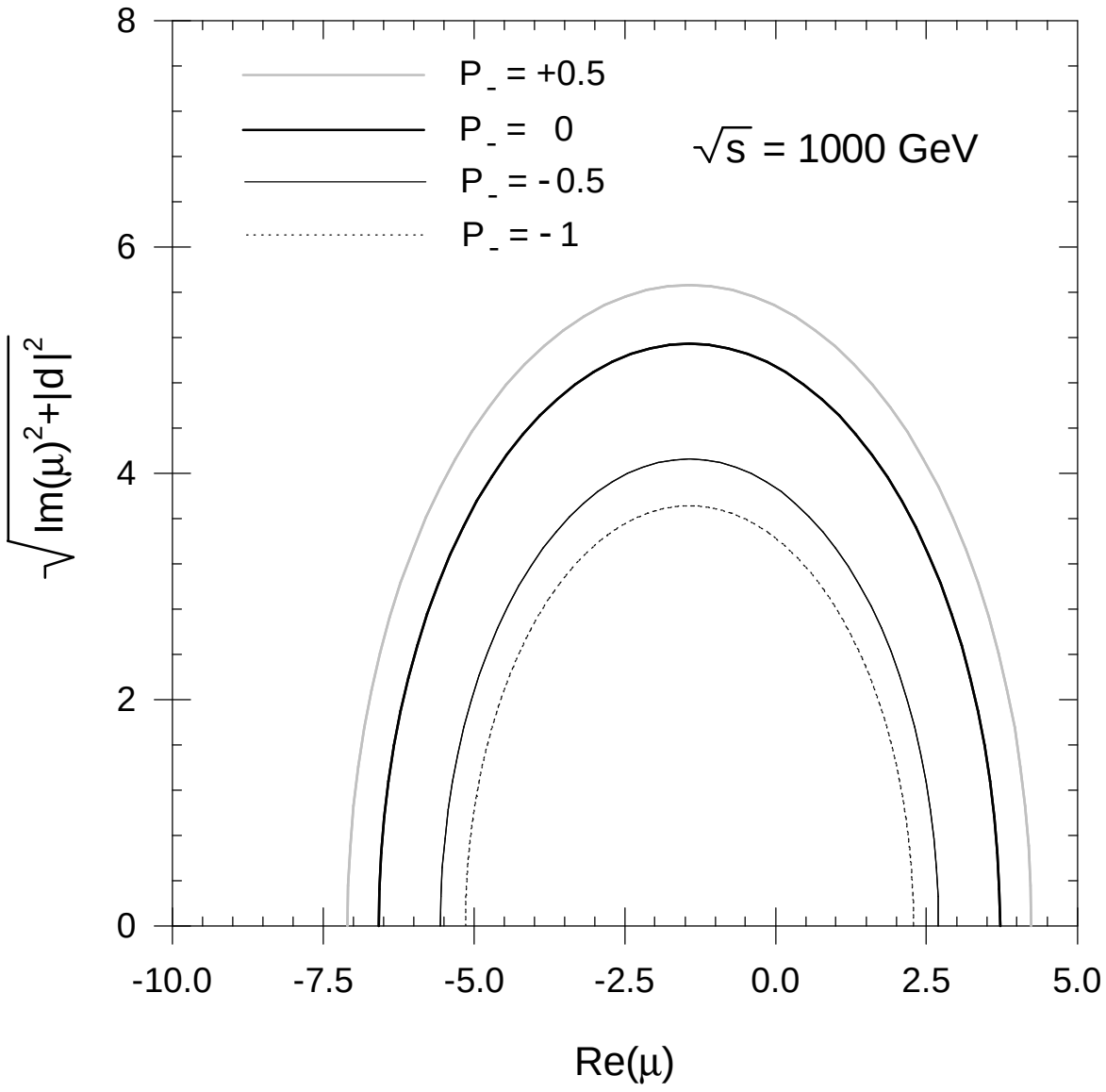

Figure 5b

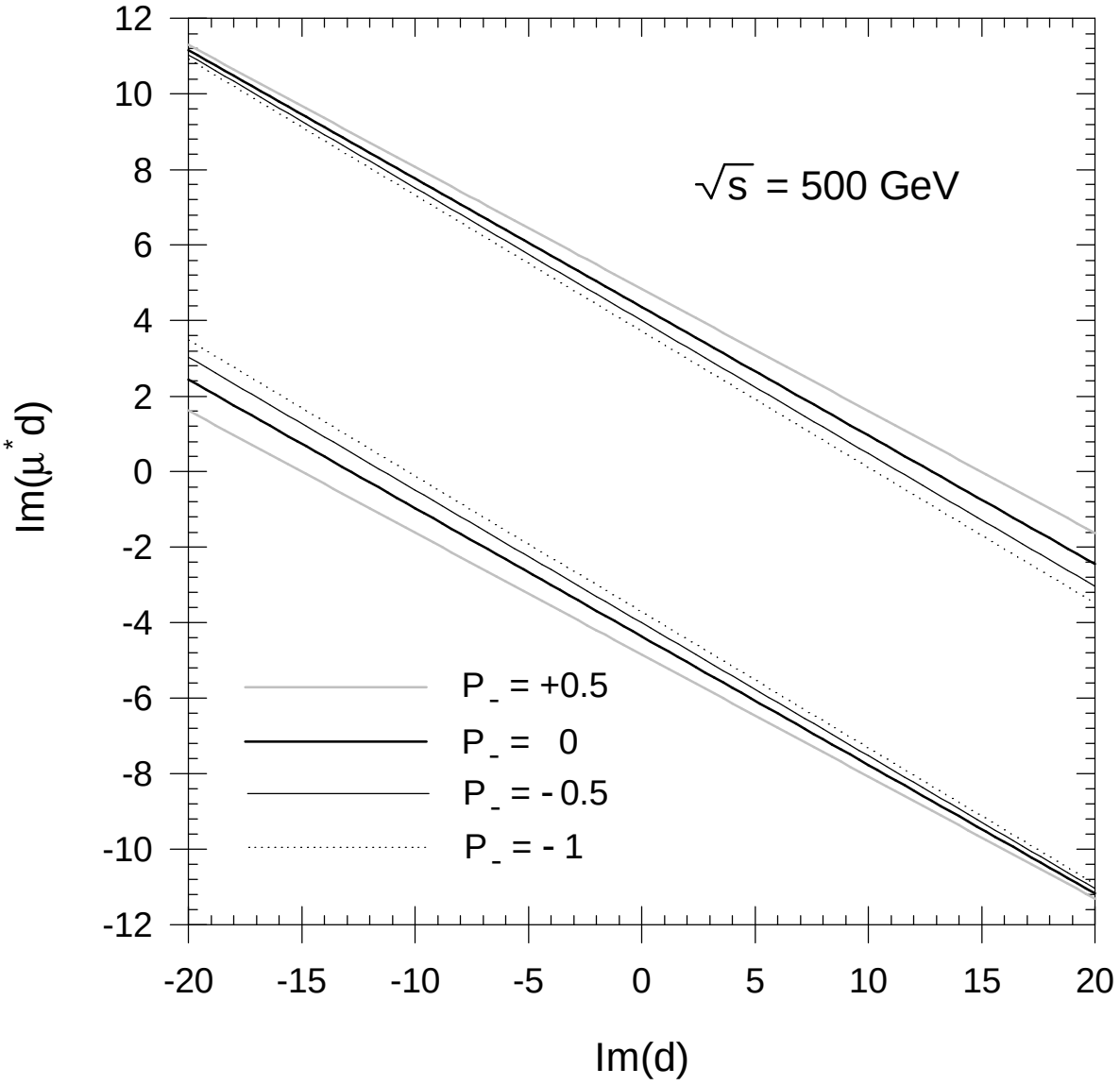
12
10
8
6
4
2
0
-2
-4
-6
-8
-10
-12
-20
-15
-10
-5
0
5
10
15
20
Im(d)
Im(μ* d)
√s = 500 GeV
P_ = +0.5
P_ = 0
P_ = - 0.5
P_ = - 1

Figure 6a

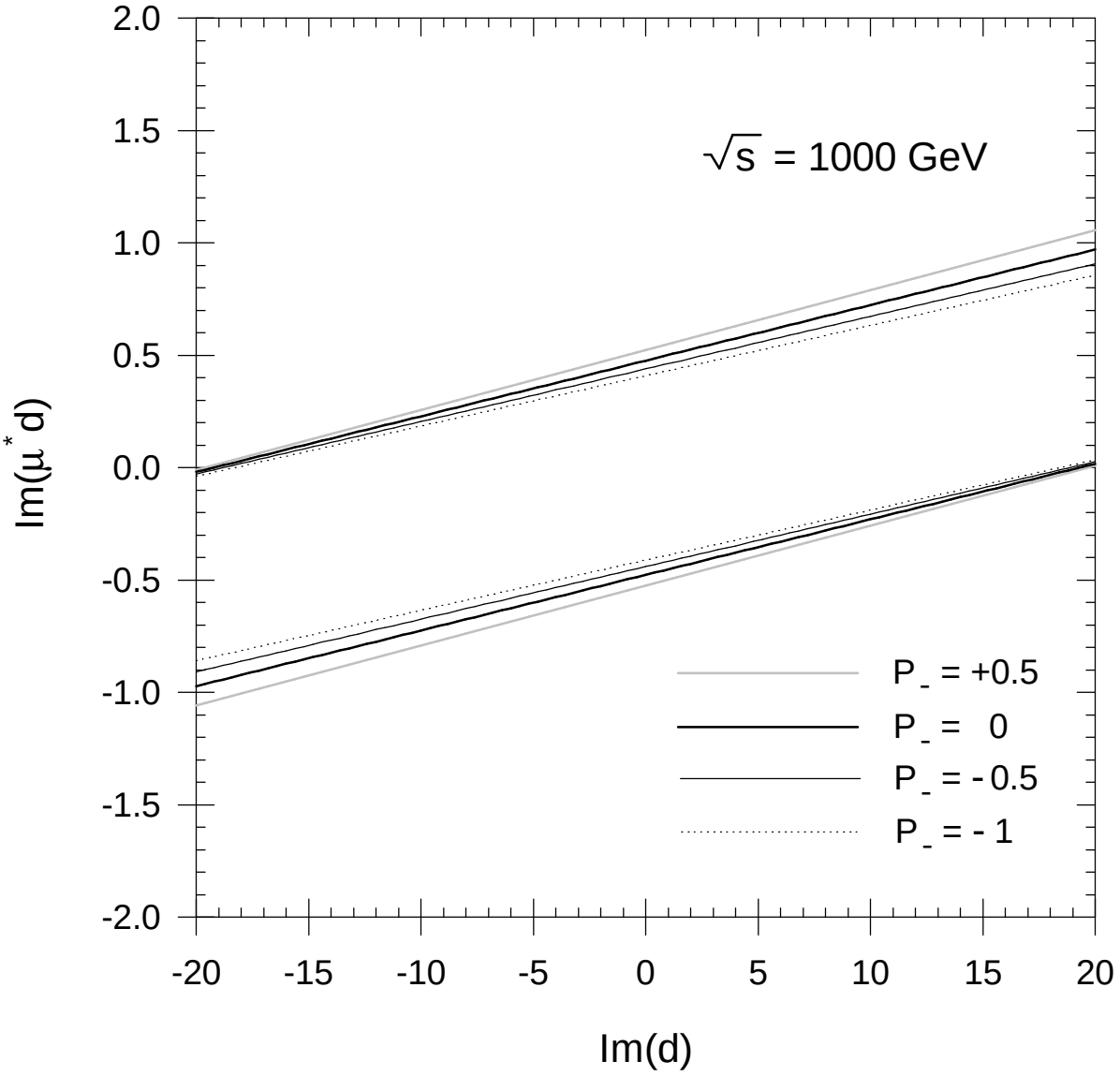
2.0
1.5
1.0
0.5
0.0
-0.5
-1.0
-1.5
-2.0
-20
-15
-10
-5
0
5
10
15
20
Im(μ* d)
Im(d)
√s = 1000 GeV
P_ = +0.5
P_ = 0
P_ = - 0.5
P_ = - 1

Figure 6b

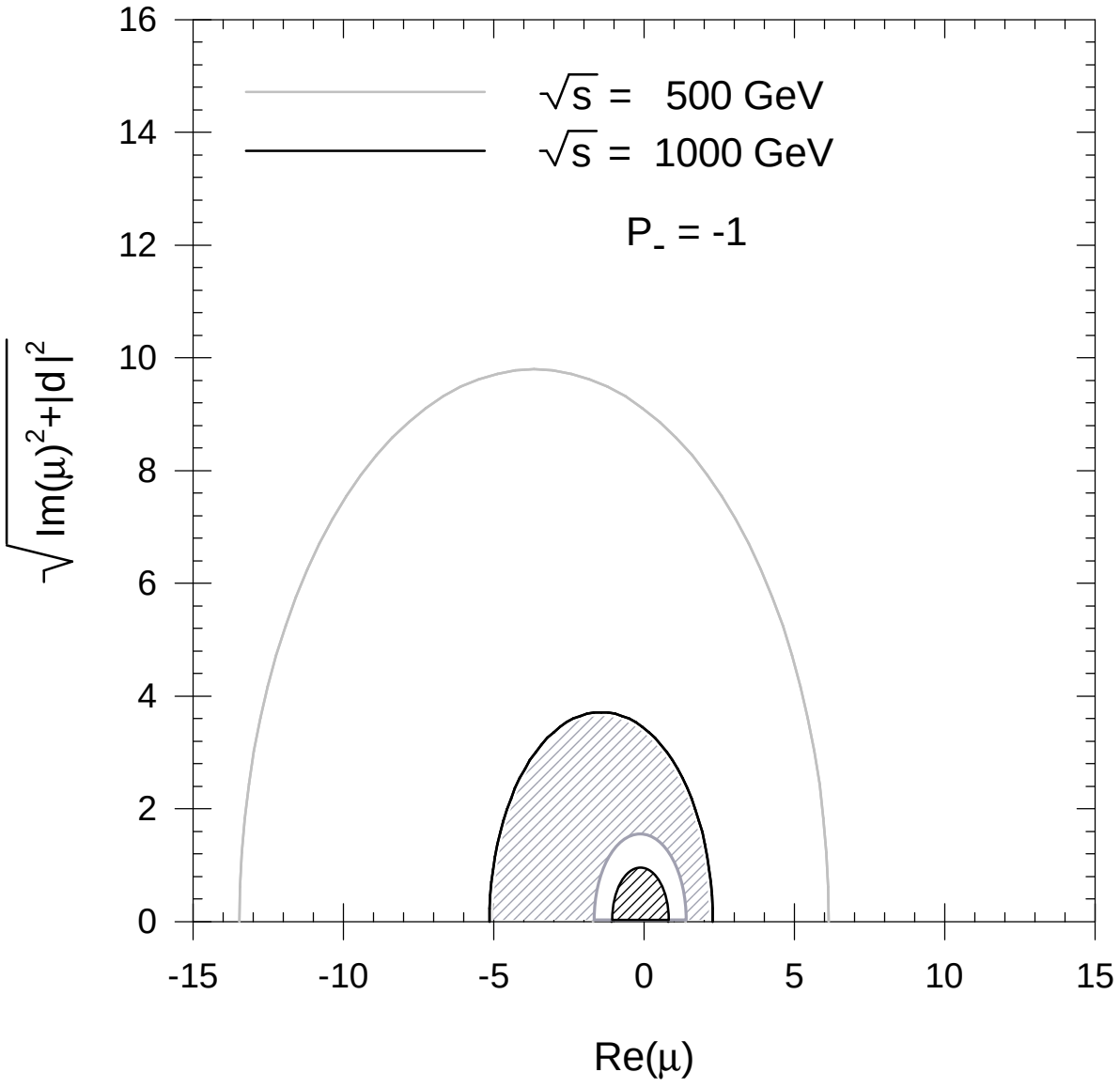
16
14
12
10
8
6
4
2
0
-15
-10
-5
0
5
10
15
√s = 500 GeV
√s = 1000 GeV
P_ = -1
√Im(μ)²+|d|²
Re(μ)

Figure 7a

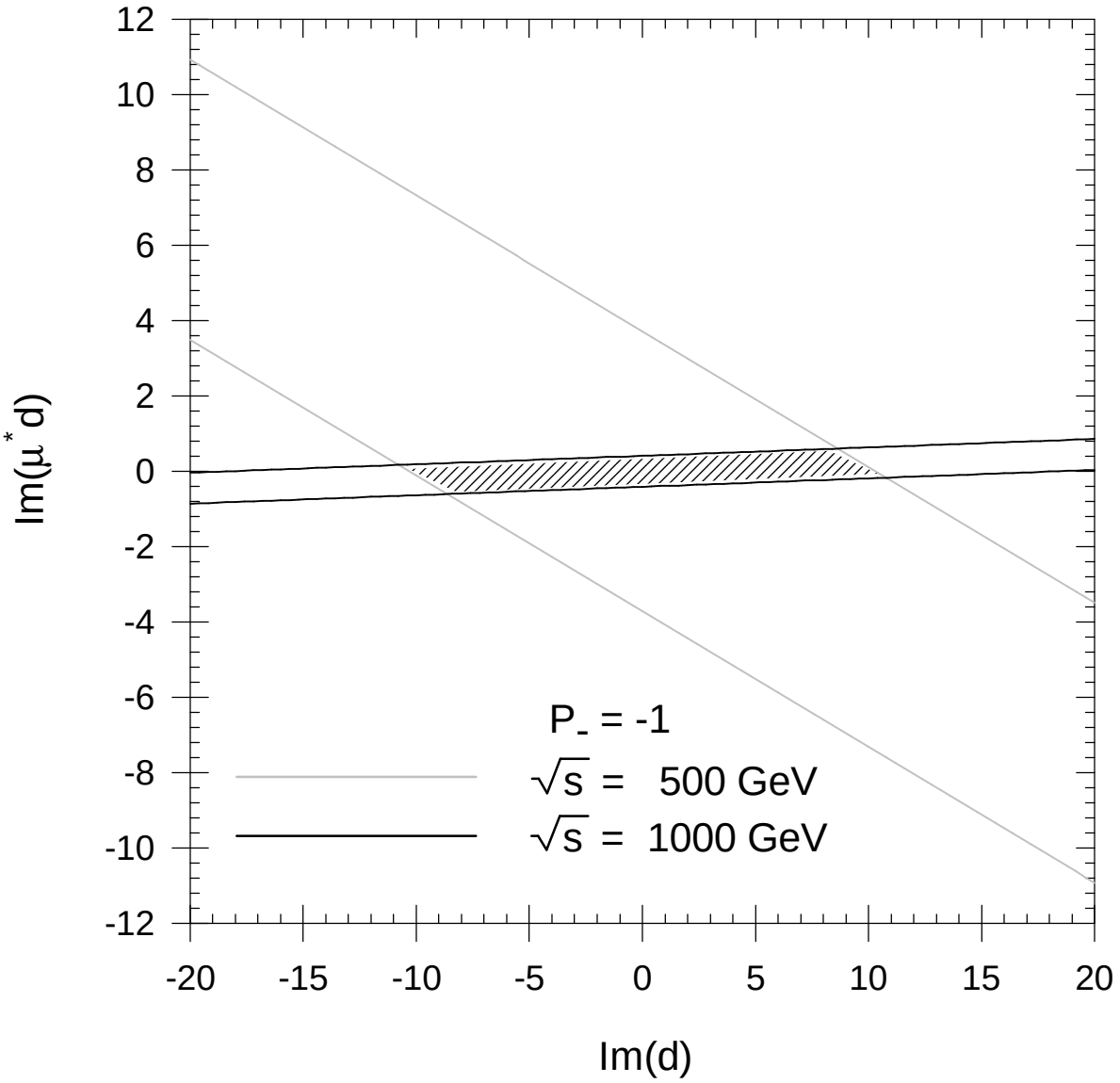
12
10
8
6
4
2
0
-2
-4
-6
-8
-10
-12
-20
-15
-10
-5
0
5
10
15
20
Im(d)
Im(μ* d)
P_ = -1
√s = 500 GeV
√s = 1000 GeV

Figure 7b